

# ZnO Growth on Si with Low-Temperature CdO and ZnO Buffer Layers by Molecular-Beam Epitaxy

F.X. XIU,<sup>1,4</sup> Z. YANG,<sup>1</sup> D.T. ZHAO,<sup>1</sup> J.L. LIU,<sup>1</sup> K.A. ALIM,<sup>2</sup>  
A.A. BALANDIN,<sup>2</sup> M.E. ITKIS,<sup>3</sup> and R.C. HADDON<sup>3</sup>

1.—Quantum Structures Laboratory, Department of Electrical Engineering, University of California, Riverside, CA 92521. 2.—Nano-Device Laboratory, Department of Electrical Engineering, University of California, Riverside, CA 92521. 3.—Center for Nanoscale Science and Engineering, Departments of Chemistry and Chemical & Environmental Engineering, University of California, Riverside, CA 92521. 4.—E-mail: xiuf@ee.ucr.edu

Low-temperature (LT) buffer-layer techniques were employed to improve the crystalline quality of ZnO films grown by molecular-beam epitaxy (MBE). Photoluminescence (PL) spectra show that CdO, as a hetero-buffer layer with a rock-salt structure, does not improve the quality of ZnO film grown on top. However, by using ZnO as a homo-buffer layer, the crystalline quality can be greatly enhanced, as indicated by PL, atomic force microscopy (AFM), x-ray diffraction (XRD), and Raman scattering. Moreover, the buffer layer grown at 450°C is found to be the best template to further improve the quality of top ZnO film. The mechanisms behind this result are the strong interactions between point defects and threading dislocations in the ZnO buffer layer.

**Key words:** ZnO, buffer layer, atomic force microscopy (AFM); photoluminescence (PL), x-ray diffraction (XRD), Raman scattering

## INTRODUCTION

With a large exciton binding energy of 60 meV, ZnO has been considered as a promising material for next-generation optoelectronic devices, such as blue-light emitting and short-wavelength laser diodes with low thresholds in the ultraviolet region.<sup>1</sup> While many researchers are focusing on fabricating p-type ZnO films, much attention has been paid to the quality of undoped ZnO films, which serve as the basis for the development of reliable and reproducible p-type films. Some native defects, such as zinc interstitials ( $Zn_i$ ) and oxygen vacancies ( $V_o$ ), are known to provide electrons to compensate holes from acceptors,<sup>2</sup> thus making p-type ZnO even harder to fabricate. Therefore, eliminating these native defects and dislocations becomes a rather important issue for the development of ZnO-based optoelectronic devices.

For potential integration with Si-based circuits and devices, the growth of high-quality ZnO film on Si is of great importance. The main obstacles to overcome, however, are large lattice mismatch and

avoiding an amorphous  $SiO_x$  layer generated in the interface, because Si is easily oxidized in oxygen environments.<sup>3</sup> To solve these problems, use of  $ZnS$ ,<sup>4</sup> Zn metal layer,<sup>5</sup>  $CdF_2$ ,<sup>6</sup> GaN,<sup>7</sup> and nitridation of Si surface<sup>8</sup> have been studied. But little progress has been made so far. Currently, low-temperature (LT) buffer-layer techniques are being paid much attention, and remarkable improvement in the crystalline quality of ZnO have been reported with various growth techniques.<sup>9–12</sup> However, optimization of buffer layers grown by MBE has not been performed, and temperature effects of buffer layers on ZnO crystalline quality have not yet been studied.

In this paper, LT-CdO-buffer- and LT-ZnO-buffer-assisted ZnO films were grown and characterized by low-temperature-photoluminescence (LT-PL), atomic force microscopy (AFM), x-ray diffraction (XRD), and Raman scattering. Temperature-dependent growth conditions for buffer layers were reported, and growth mechanisms were analyzed.

## EXPERIMENTAL PROCEDURES

ZnO films were grown on Si (100) with LT CdO and ZnO buffer layers by an electron cyclotron resonance

(ECR)-assisted MBE. Elemental zinc (5N), cadmium (6N), and oxygen gas (5N) were used as molecular beam sources. Zinc and cadmium were evaporated by LT effusion cells. Oxygen plasma was generated by an ECR plasma source. Si (100) substrates are n-type wafers with resistivity of 20–30  $\Omega$  cm. All of these substrates were cleaned by the Piranha-HF method and dried with nitrogen gas.

During growth, several steps were followed. In step I, Si substrates were thermally cleaned at 650°C for 10 min. In step II, CdO and ZnO buffer layers were deposited on Si at different growth temperatures of 350, 450, and 550°C. In step III, ZnO films were grown on top of buffer layers at 550°C. For all these samples, growth conditions for top ZnO films remained the same while growth temperatures of the buffer layers were different, as shown in Table I. In addition, a ZnO film without a buffer layer was grown directly on a Si substrate for comparison with the samples mentioned above.

PL spectra were measured by the excitation from a 325-nm He-Cd laser at 8 K. A Nanoscope III AFM was employed to study surface morphologies. A Bruker Advanced D8 x-ray diffractometer was utilized to investigate ZnO crystalline quality. A  $\theta$ – $2\theta$  scan was performed to determine growth orientations. A Renishaw micro-Raman spectrometer 2000 with visible (488 nm) excitation lasers was used to measure Raman scattering spectra at room temperature.

## RESULTS AND DISCUSSION

We have attempted to use CdO as a hetero-buffer layer to improve ZnO crystalline quality. LT-PL measurements were carried out at 8 K to study optical properties of ZnO/CdO/Si films, as shown in Fig. 1. Strong near-band-edge UV emissions associated with neutral-donor-bound excitons ( $D^{\circ}X$ ) are observed at 3.355 eV, which are attributed to native defects ( $V_o$  and  $Zn_i$ )<sup>2</sup> and/or H incorporation.<sup>13</sup> For samples with CdO buffers (samples a–c), however, broad peaks between 2.80 and 3.20 eV are found besides  $D^{\circ}X$  emissions. These peaks are mainly associated with nonradiative recombination centers in the forbidden gap of ZnO as a result of high-density dislocations in these films. In addition, some Cd atoms might diffuse into top ZnO layers during growth; therefore a thin layer of CdZnO could be developed in the interface between ZnO and CdO, contributing

to these peaks. Moreover, when compared with those from sample (d), the full-width at half-maximum (FWHM) values remain the same after employing CdO buffer layers, indicating that CdO layers with a temperature region of 350–550°C and a thickness of 0.5  $\mu$ m may not be ideal conditions for improving ZnO crystalline quality.

Figure 2 shows PL spectra (at 8 K) for ZnO films with homo-buffer layers grown at (e) 450°C, (f) 350°C, and (g) 550°C, respectively. Sample (d) is a ZnO film directly grown on a Si substrate. For all samples, strong near-band-edge UV emissions are observed at 3.355 eV. When compared with sample (d) (28.3 meV), the films with LT ZnO-buffers (samples e–g) have much smaller FWHM values, 12, 22.5, and 22.7 meV, respectively, indicating improvement in crystalline quality. Furthermore, sample (e) shows no pronounced deep-level defect-related emissions, suggesting the best crystalline quality of ZnO film obtained with use of a 450°C buffer layer.

Surface morphologies and structural properties of ZnO films were investigated by AFM and XRD, respectively. Characterized by AFM, root-mean-square (RMS) roughness for samples (d)–(g) are 6.8, 3.3, 6.7, and 7.4 nm, respectively. Among them, sample (e) shows a dramatic improvement of surface morphology by using a 450°C buffer layer. Figure 3 shows typical XRD  $\theta$ – $2\theta$  spectra of these ZnO films (samples d–g). It is well known that ZnO films are usually grown with  $c$ -axis preferred orientation under typical growth conditions. This is because of the lowest surface energy of the (001) basal plane in ZnO, which leads to preferred growth in the (001) direction.<sup>14</sup> Consistent with this theory, all of the samples in our experiments exhibit a preferred orientation of (002). However, ZnO films with buffer layers (samples e–g) show much higher diffraction intensity than the film without a buffer layer (sample d), which indicates the marked improvement of crystalline quality of ZnO films by employing ZnO buffer layers. Moreover, sample (a), with a buffer layer grown at the intermediate temperature of 450°C, shows the smallest FWHM value of 0.209° as well as the highest diffraction intensity, which is in good agreement with previous LT-PL and AFM analyses. It is also noted that the 350°C buffer sample (f) has another growth orientation (101). It is believed that, at low temperature, not all zinc and oxygen atoms can migrate effectively and diffuse

Table I. Growth and Structural Data of ZnO Films

Sample <sup>a</sup>	Buffer Layer	Thickness ( $\mu$ m)	Buffer-Layer Growth Temperature (°C)	Active ZnO Layer Thickness ( $\mu$ m)
a	CdO	0.5	450	0.7
b	CdO	0.5	350	0.7
c	CdO	0.5	550	0.7
e	ZnO	1.1	450	0.7
f	ZnO	1.1	350	0.7
g	ZnO	1.1	550	0.7

<sup>a</sup> Sampled is a ZnO film directly grown on Si at 550°C without buffer layers.

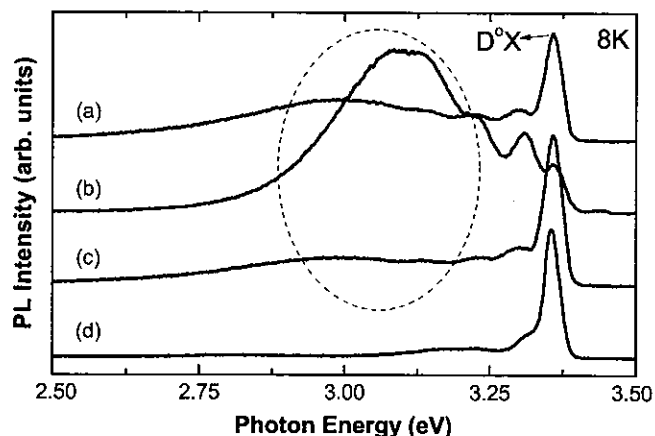


Fig. 1. PL spectra (at 8 K) of ZnO/CdO/Si samples with CdO buffer layers grown at (a) 450°C, (b) 350°C, and (c) 550°C. Sample (d) is a ZnO film directly grown on a Si substrate. The circular area represents the PL emissions from defect-related deep levels and CdZnO thin layers.

into other crystalline grains. Therefore, crystalline grains with other orientations, such as (101), can be developed.

Figure 4 shows the typical Raman spectra. ZnO characteristic peaks are observed at 436.5, 438.6, 438.6, and 438.6  $\text{cm}^{-1}$ , for samples (d)–(g), respectively. These peaks are assigned to  $E_2$  vibration modes of ZnO, which are related to a band characteristic of a wurtzite phase. It is well known that ZnO has the wurtzite structure and belongs to the space group  $C_{6v}^4$ . According to group theory, there are two  $A_1$ , two  $E_1$ , two  $E_2$ , and two  $B_1$  modes. Only the two  $B_1$  modes are not Raman active. For highly oriented ZnO films, if the incident light is perpendicular to the surface of films, only the  $E_2$  modes and the  $A_1$  (LO) mode are expected to be observed, while the other modes are forbidden according to Raman selection rules.<sup>15</sup> It was obvious that the intensity of the  $E_2$  mode reached the highest value and FWHM is the smallest when a buffer layer was grown at 450°C (sample e). Because the thickness of these ZnO films is less than the light penetration

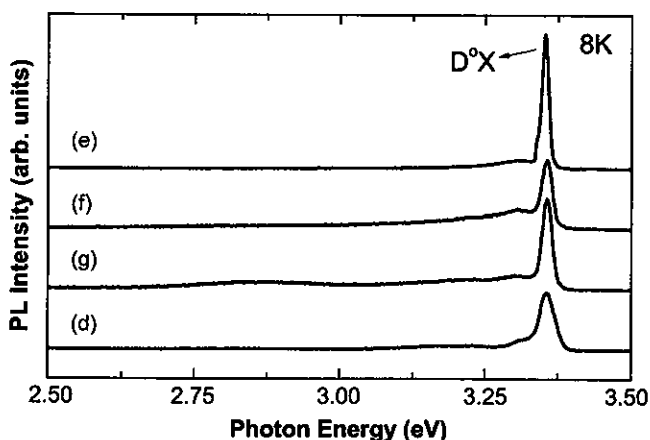


Fig. 2. PL spectra (at 8 K) of ZnO/ZnO/Si samples with ZnO buffer layers grown at (e) 450°C, (f) 350°C, and (g) 550°C. Sample (d) is a ZnO film directly grown on a Si substrate.

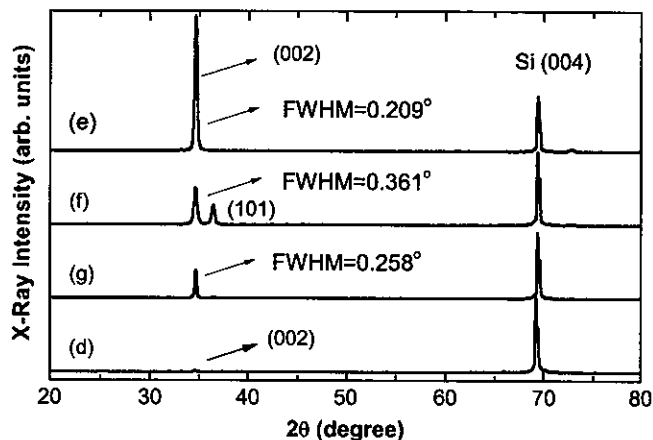


Fig. 3. RT XRD spectra of ZnO/ZnO/Si samples with ZnO buffer layers grown at (e) 450°C, (f) 350°C, and (g) 550°C. Sample (d) is a ZnO film directly grown on a Si substrate.

depth,  $E_2$  (high) modes of Si substrate are observed at a frequency of 520.6  $\text{cm}^{-1}$ , which was also reported by Ye et al.<sup>16</sup>

The growth mechanisms are interpreted based on two assumptions. First, the quality of high-temperature (HT) ZnO film depends on the quantity of threading dislocations that can penetrate the buffer layer and reach the top HT ZnO film. Second, the buffer layers inevitably generate different amounts of point defects at different growth temperatures, which can interact with these dislocations; specifically they can cause dislocations to climb, which helps to annihilate threading dislocation arms with opposite Burgers vectors.<sup>17</sup> Therefore, the quality of the top ZnO film depends on the interactions of point defects with threading dislocations in the buffer layer. At low temperatures (such as 350°C), oxygen and zinc atoms do not gain enough energy to migrate and diffuse into the neighboring area. Therefore, large-density point defects are generated and the film is isotropic. In this case, interactions between point defects and threading dislocations are negligible due to the isotropy of the buffer layer. At high temperatures (such as 550°C), only

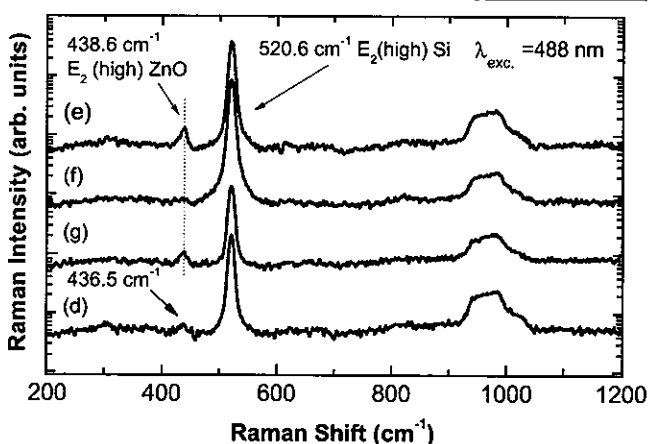


Fig. 4. RT Raman spectra of ZnO/ZnO/Si samples with ZnO buffer layers grown at (e) 450°C, (f) 350°C, and (g) 550°C. Sample (d) is a ZnO film directly grown on a Si substrate.

a small amount of point defects is generated. The interactions between point defects and threading dislocations are so weak that most threading dislocations cannot annihilate each other and therefore easily pass through point defects to reach the top active layer. At intermediate temperatures (such as 450°C), however, the amount of point defects is generated in such a way that many threading dislocations strongly interact with point defects, resulting in the annihilation of dislocation arms. Therefore, the crystalline quality of the top HT ZnO is much better.

### CONCLUSIONS

In summary, we have employed CdO and ZnO as buffer layers prior to ZnO growth to improve the film quality. LT-PL spectra show that CdO, as the hetero-buffer layer, does not improve ZnO layer quality on top. However, by using ZnO as the homo-buffer layer, the crystalline quality can be greatly enhanced, as indicated by PL, AFM, XRD, and Raman spectra. Moreover, the buffer layer temperature of 450°C was found to be the best condition to enhance the crystalline quality of ZnO film on top. The mechanism behind is the generation of point defects in the LT growth condition, which interacts with threading dislocations to reduce its density in the top active ZnO films.

### ACKNOWLEDGEMENT

This work was supported by DARPA/DMEA through the center for NanoScience and Innovation

for Defense (CNID) under award number H94003-04-2-0404.

### REFERENCES

1. D.C. Look, B. Claffin, Ya.I. Alivov, and S.J. Park, *Phys. Status Solidi (a)* 201, 2203 (2004).
2. S.B. Zhang, S.H. Wei, and A. Zunger, *Phys. Rev. B: Condens. Matter Mater. Phys.* 63, 075205 (2001).
3. M. Fujita, N. Kawamoto, M. Sasajima, and Y. Horikoshi, *J. Vac. Sci. Technol., B* 22, 1484 (2004).
4. A. Miyake, H. Kominami, H. Tatsuoka, H. Kuwabara, Y. Nakanishi, and Y. Hatanaka, *J. Cryst. Growth* 214/215, 294 (2000).
5. N. Kawamoto, M. Fujita, T. Tatsumi, and Y. Horikoshi, *Jpn. J. Appl. Phys.* 42, 7209 (2003).
6. M. Watanabe, Y. Maeda, and S.I. Okano, *Jpn. J. Appl. Phys.* 39, L500 (2000).
7. A. Nahhas, H.K. Kim, and J. Blachere, *Appl. Phys. Lett.* 78, 1511 (2001).
8. K. Iwata, P. Fons, S. Niki, A. Yamada, K. Matsubara, K. Nakahara, T. Tanabe, and H. Takasu, *J. Cryst. Growth* 214/215, 50 (2000).
9. D.Y. Lee, C.H. Choi, and S.H. Kim, *J. Cryst. Growth* 268, 184 (2004).
10. T. Nakamura, Y. Yamada, T. Kusumori, H. Minoura, and H. Muto, *Thin Solid Films* 411, 60 (2002).
11. K. Ogata, T. Kawanishi, K. Maejima, K. Sakurai, S.Z. Fujita, and S.G. Fugita, *J. Cryst. Growth* 237, 553 (2002).
12. S.H. Jeong, I.S. Kim, J.K. Kim, and B.T. Lee, *J. Cryst. Growth* 264, 327 (2004).
13. C.G. Van de Walle, *Phys. Rev. Lett.* 85, 1012 (2000).
14. S.S. Kim and B.T. Lee, *Thin Solid Films* 446, 307 (2004).
15. T.C. Damen, S.P.S. Porto, and B. Tell, *Phys. Rev.* 142, 570 (1966).
16. J.D. Ye, S.L. Gu, S.M. Zhu, T. Chen, W. Liu, F. Qin, L.Q. Hu, R. Zhang, Y. Shi, and Y.D. Zheng, *J. Vac. Sci. Technol., A* 21, 979 (2003).
17. E. Kasper, K. Lyutovich, M. Bauer, and M. Oehme, *Thin Solid Films* 336, 319 (1998).